

Supporting Information

# Role of 4-*tert*-Butylpyridine as a Hole Transport Layer Morphological Controller in Perovskite Solar Cells

*Shen Wang, <sup>†</sup>|| Mahsa Sina, <sup>†</sup>|| Pritesh Parikh, <sup>†</sup> Taylor Uekert, <sup>†</sup> Brian Shahbazian, <sup>†</sup> Arun Devaraj, <sup>‡</sup> Ying Shirley Meng <sup>†\*</sup>*

<sup>†</sup> Department of NanoEngineering, University of California San Diego, 9500 Gilman Drive, La Jolla, CA 92093, USA

<sup>‡</sup> Physical and Computational Sciences Directorate, Pacific Northwest National Laboratory, P.O. Box 999, Richland, Washington 99352, USA

\* E-mail (Y.S.M.) shirleymeng@ucsd.edu

## Methods

All reagents, unless otherwise stated, were purchased from Sigma-Aldrich.

*Methylammonium iodide (MAI) synthesis:* 15 mL of 33 wt% methylamine solution in anhydrous methanol was reacted with 15 mL of 57 wt% hydroiodic acid in a flask for 1 hour. After evaporating all solvents, the mixture was dissolved in anhydrous ethanol. Ethyl ether was used to precipitate MAI from the solution. The MAI was dried overnight in a vacuum oven, and a white crystalline powder was obtained as the final product.

*Perovskite solar cells (PSCs) fabrication:* PSC fabrication was based on the sequential deposition method.<sup>1</sup> A TiO<sub>2</sub> compact layer was spin-coated on cleaned FTO glass. After sintering, a mesoporous TiO<sub>2</sub> layer was spin-coated onto the TiO<sub>2</sub> compact layer and sintered again. PbI<sub>2</sub> (Alfa Aesar) was dissolved in dimethyl formamide and spin-coated onto mesoporous TiO<sub>2</sub>. Then the films were dipped in MAI solution (isopropanol as the solvent). After thermal annealing, the films were spin-coated with a solution containing Spiro-OMeTAD (Merck), tBP, and LiTFSI which were dissolved in chlorobenzene. Finally 80 nm of gold was evaporated onto the films. For more detailed information (spin-coating speed/time, solution concentration, and annealing condition) see reference.<sup>2</sup>

### *Characterization:*

Scanning Electronic Microscopy (SEM) images were taken with a FEI SFEU UHR SEM operated at 10kV. Samples were coated with iridium before taking SEM images to avoid beam drift for semiconducting and insulating materials.

Transmission electron microscopy (TEM) images were taken with a FEI 200kV Sphera Microscope. Samples for TEM were prepared by focused ion beam (FEI Scios DualBeam FIB/SEM). Regions of interest were deposited with 2 um thick Pt for protection during ion etching. After etching from the substrate, the samples were lifted by a tungsten needle (FEI EasyLift LT NanoManipulator). Before disconnecting the sample from the needle, samples were attached onto the FIB lift-out grid (Copper PELCO FIB Lift-Out Grid). Subsequently samples attached onto the lift-out grid were thinned to within 100 nm by a Ga<sup>2+</sup> ion beam. In addition, the EFTEM images and EELS spectra were acquired using a Gatan Enfina spectrometer with a collection angle of 52 mrad and convergence angle of 30 mrad.

Samples for atom probe tomography (APT) were prepared and analyzed at the Environmental and Molecular Sciences Laboratory at PNNL.

In brief samples were prepared from fabricated PSC devices, in the form of tips, using FEI Helios dual-beam focused ion beam/scanning electron microscope (FIB/SEM) equipped with an Omniprobe. A wedge shaped lift-out section was prepared by milling at 22 degrees. The liftout section was controlled using an in-situ micromanipulator (Omniprobe) and 2  $\mu$ m sections were cut and affixed on a Si microtip array followed by Pt deposition on either side to hold the wedge in place. An annular milling pattern with progressively smaller diameter was used to get the shape

of a tip. A final low beam energy (~ 2kV) exposure was used to give the tip its final shape as well as remove surface regions, which are prone to maximum Ga damage. The end radius at the tip was less than 100 nm.

As prepared sample tips were then analyzed using a LEAP (local electrode atom probe) 4000XHR with a detector efficiency of ~40%. A temperature of 60 K and laser energy (~ 100 pJ) was used to ensure field evaporation of ions in a regular manner. The laser energy, detection rate and temperature were optimized for our samples. The reconstruction to obtain the 3-D maps and the analysis were done using the IVAS® software.

Fourier transform infrared spectroscopy (FTIR) with attenuated total reflectance (ATR) attachment (Nicolet 6700 with Smart-iTR) was applied for the FTIR test. Samples for FTIR were spin-coated on CaF<sub>2</sub> substrates at 2000 r.p.m. and 30 s as thin films.

### **Supplementary Data**

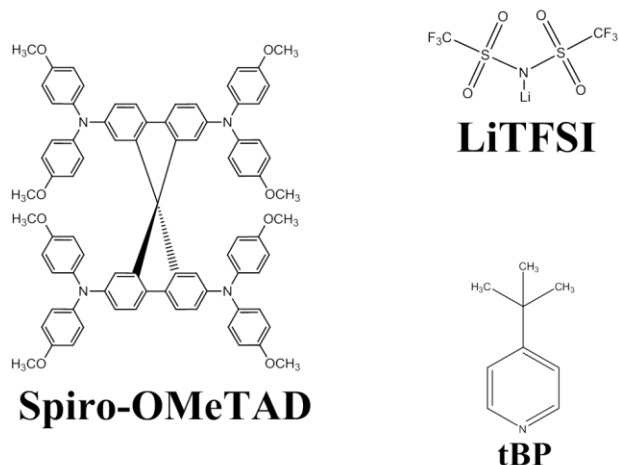


**Figure S1.** Molecular Structures of the components in the HTL for PSCs: Spiro-OMeTAD, LiTFSI and tBP.

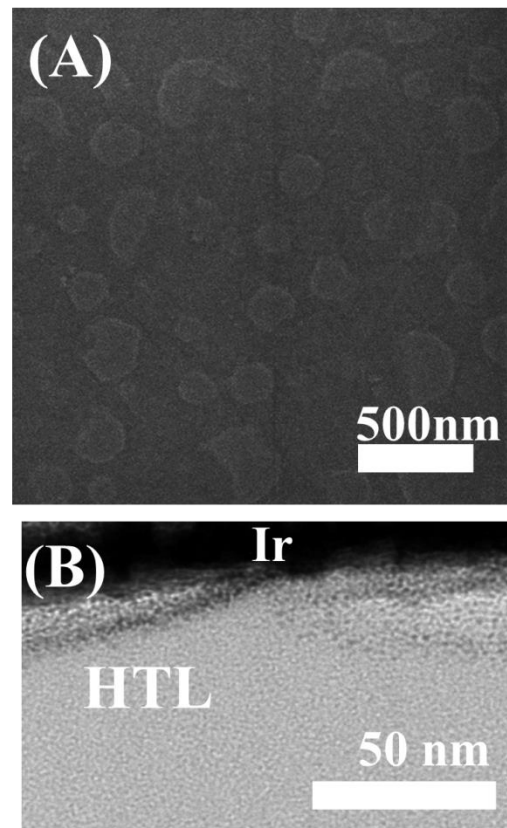


**Figure S2.** (A) Top-view SEM images of the freshly prepared HTL with tBP after thermal annealing treatment. (B) Cross-section BF-TEM images of the freshly prepared HTL with tBP after thermal annealing treatment.

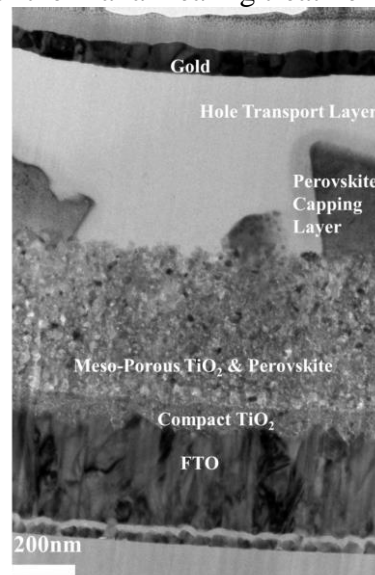


**Figure S3.** Cross-section BF-TEM image of a PSC, which indicates that the HTL has a homogeneous morphology. The sample was intentionally prepared with less perovskite coverage in order to display more HTL area.

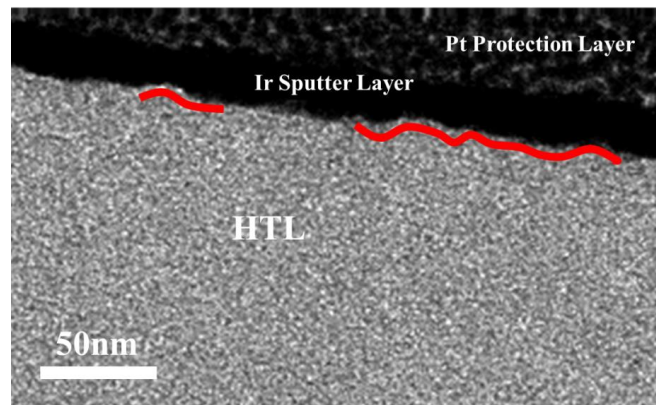


**Figure S4.** Cross-section BF-TEM image of the HTL with a metal capping layer. It reveals the curved structure of the HTL/metal interface. The red line marks the curved portions of the interface. The sample was prepared by FIB.

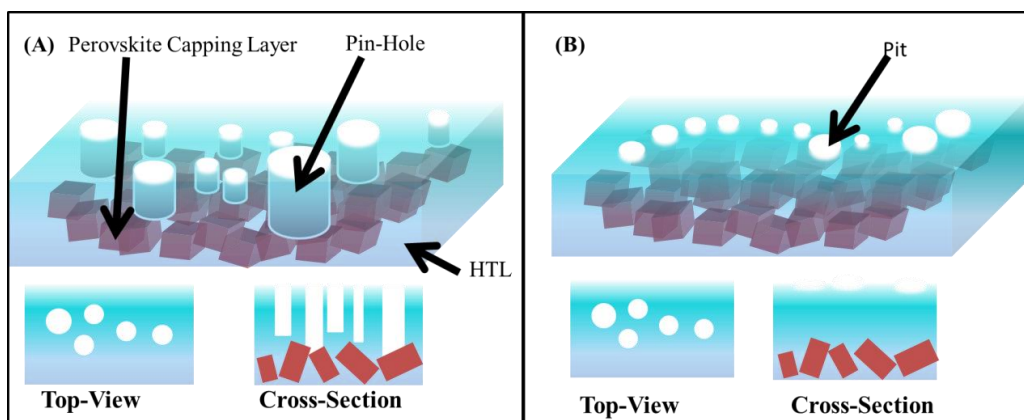


**Figure S5.** Schematic of the HTL with a perovskite capping layer (A) pin-hole model; (B) pit model. They have similar top-view morphology, but the cross-section morphology is clearly distinguishable.

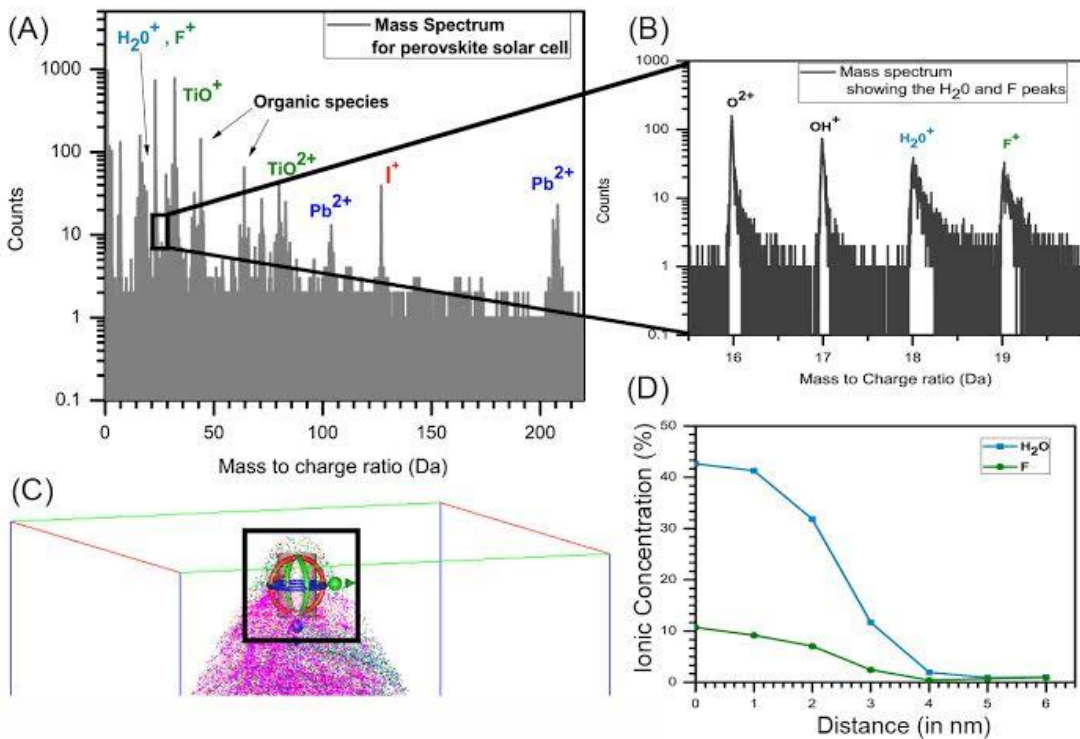


**Figure S6.** Additional analysis for atom probe tomography performed on perovskite solar cells. (A) Shows the mass spectrum for the analysis region shown in **Figure 7** main text. (B) Zoom in of the mass spectrum for the region marked by the black box in (A). The peak for  $\text{H}_2\text{O}$  is clearly visible. The high intensity of this peak does not fit the isotopic ratios as expected for  $\text{O}^{2+}$ . (C) The analysis region (marked by the black box) for the 1-D concentration profile. (D) 1-D concentration profile showing the decrease in  $\text{F}$  and  $\text{H}_2\text{O}$  species across the interface.

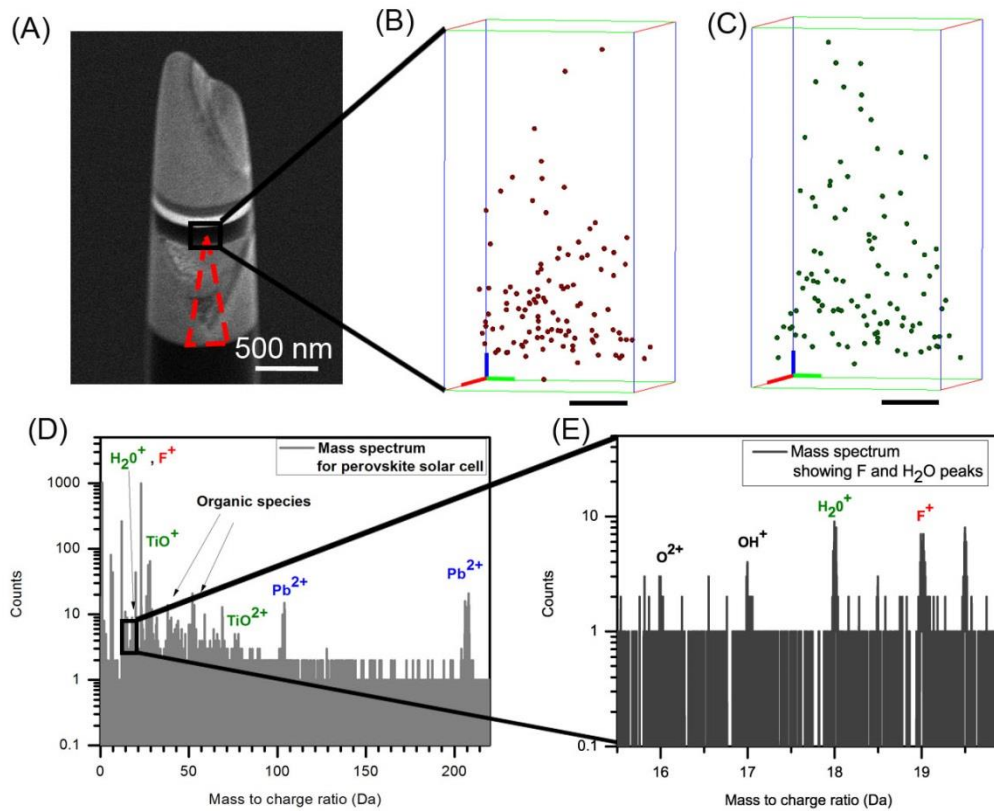


**Figure S7.** Analysis for atom probe tomography performed on freshly prepared perovskite solar cells (cells that were prepared into tips and analyzed right after device preparation to prevent influence of moisture). (A) Shows the SEM image for the analysis region with tip going from the hole transport layer into the perovskite layer. (B) APT map of F (fluorine) showing its distribution in 3D (C) APT map of H<sub>2</sub>O showing its distribution in 3D. (Scale bar in (B) and (C) are 8 nm. Shown in green is the x-axis, red corresponds to the y-axis and blue is the z-axis.) (D) Shows the mass spectrum for the analysis region shown in (A). (E) Zoom in of the mass spectrum for the region marked by the black box in (D). The peak for H<sub>2</sub>O is clearly visible. The high intensity of this peak does not fit the isotopic ratios as expected for O<sup>2+</sup>. In comparison to Figure S6 (B) the maximum ionic count for both F and H<sub>2</sub>O are 5 times lower in the freshly prepared sample, validating the role of tBP both as an agent to improve miscibility and reduce the moisture content of the hole transport layer.

### Supplementary Reference

- (1) Burschka, J.; Pellet, N.; Moon, S.-J.; Humphry-Baker, R.; Gao, P.; Nazeeruddin, M. K.; Gräzel, M. *Nature* **2013**, *499*, 316–319.
- (2) Wang, S.; Yuan, W.; Meng, Y. S. *ACS Appl. Mater. Interfaces* **2015**, *7*, 24791–24798.